NEW CONCEPT FOR IMPROVING SOLAR STILL PERFORMANCE BY USING VIBRATORY HARMONIC EFFECT THEORETICAL ANALYSIS, PART-2

Khaled M. S. Eldalil

Dr., Part time Lecturer, Mech. Eng. Dept, Tanta University, Tanta, Egypt
and R&D Consultant, Egypt and Saudi Arabian
E-mail: eldalil01@msn.com

ABSTRACT

This paper presents the theoretical analysis of a new concept basin type solar still with added helical wires packing layer subjected to a vibratory effect. The improvement of the performance of this basin type solar still is described in details experimentally in part-1, by the author. The thermal modeling have been done by using the imperial relations of the free convection heat transfer in order to correlate the temperature difference of the thermal boundary layer in the basin water depth in both flat bottom and with added helical wire packing layer. The system dynamics is modeled based on the transmissibility equation for evaluating the periodic motions of the helical wired packed layer and the condensing polycarbonate glass cover. The effect of these harmonic motions on the heat transfer coefficient is correlated. The effect due to added helical wired packed layer with and without vibration is compared with the conventional basin type solar still (CSS) and the experimental results obtained in Part-1 by the author and come in good agreement. The deviation of the theoretically calculated results is found about +7% and +11.1% at low and high basin water temperatures respectively.

Keywords: Vibratory effect, harmonic motion, helical wired packed layer, transmissibility.

1. INTRODUCTION

Distilled water is needed for drinking, irrigation and for many other applications. A diversity of approaches are used for these portions of fresh water from saline water; namely multi stage flash (MSF), multiple effect (ME), reverse osmosis (RO), electro-dialysis, ion exchange, phase change, and solvent extraction. These methods are expensive, however, for the production of small amount of fresh water. The development of solar distillation has demonstrated its suitability for the desalination process when the weather conditions are suitable and the demand is not too large, i.e. less than 200 m³/d. The problem of low daily productivity of the solar stills triggered scientists to investigate various means of improving the stills productivity and thermal efficiency.

Different aspects of triangular-shaped solar stills (CSS), also called double slope stills, have been studied. Production in this still is influenced by the orientation, as shown by Singh et al. [2], who found the maximum yield for a cover with east–west. Detailed studies of heat transfer coefficients can also be found, Sharma, Mullick [3], in which energy transfer mechanisms, such as convection, evaporation and radiation are investigated, and new empirical relations to estimate cover temperatures are proposed. To model heat and mass transfer in solar stills, Dunkle [4] proposed the use of a correlation of the form Nu $=CR^n$ where C is 0.075 and n is 1/3 for air enclosed between horizontal parallel plates. This correlation is expressed in terms of a modified temperature difference that includes molecular weight and buoyancy, and considers the cover as a single element. This has been the most widely accepted model for solar stills and describes the basic heat and mass transport mechanism between heated water mass and a condenser.

Numerous studies on solar stills of various designs to increase its productivities and efficiencies have been carried out theoretically and experimentally. The theoretical studies include the determination of the dependence of the productivity on weather, the construction design, and operation parameters. Followed by others, Mowla and Karimi, [5] they presented a mathematical simulation study for a solar still rate of production of fresh water from sea water as a function of different meteorological parameters and the solar still specifications, their model is overestimated in calculating the daily production. Aboul-Enein et al. [6] investigated the thermal performance of the still both experimentally and theoretically. They presented a simple transient mathematical model for the solar still based on the analytical solution of the energy-balance equations for different parts of the still and analytical expressions for temperatures of different components. Good agreement between experimental and theoretical results is observed.

Tiwari and Noor [7] presented a transient analysis of a conventional solar still and the derivation of suitable parameters to assist in the characterization of various designs of solar stills and giving a methodology to test and compare the various designs of solar stills, they concluded that there is good agreement between experimental and theoretical results.

Modified solar stills are also investigated by Tanaka et al. [8,9], presented a theoretical parametric study on a vertical multiple-effect diffusion-type solar still consisting of a flat plate reflector, a number of vertical parallel partitions in contact with saline-soaked wicks with narrow air gaps between partitions, to determine the effect of these factors that could cause a decrease in the distillate productivity of the still. They obtained mathematical models describing the heat transfer process and performance of the solar still productivity.

Zeinab et al. [10] presented an experimental and analytical study for a new active technique by using rotating shaft together with adding special packed thermal layer; it is formed from glass balls which are considered a simple thermal storage system.

In this work, the effect of the modified packed layer on the performance of the solar still is correlated and the interaction with the vibratory harmonic effect is modeled using Dunkle [4] model and results obtained by Eduardo Rubio-Cerda et al. [11] and modified by Fatani and Zaki [12] to account for evaporative heat transfer as general formula for the conventional solar still (CSS) performance, also, by utilizing the empirical relations of the convective heat transfer together with the convection-turbulent in the case of vibratory effect.

1.1. Solar Still Description

This theoretical work is concerned to the active solar still which is described in details in part-1, Eldalil [1], it designed and built in the southern desert area of Saudi Arabia (Wadi El-dwaser, 21.5° latitude and 44° longitude), in the year 2006 to supply distillate water to a battery service center in a large farm. It uses the under ground water as a brine, which is lifted from deep wells.

The system has a double sloped cover of 30° inclination with the horizontal and total effective area of 2.064 m². It is made from coated steal sheets and steel sections; Figure (1) shows a schematic drawing of the solar still. The transparent cover is made from polycarbonate composite sheets of 4 mm thickness partitioned to six segments, three on each side. A tight sealing of the inside enclosure is attained by using silicon rubber past with galvanized bolts for all connections of top cover and basin parts.

Helical copper wires are stretched over the basin bottom, as shown in Figure (2). The coil mean diameter is 25 mm and the wire diameter is 1.5 mm, they are blackened as the basin bottom. The average depth of the brine water in the basin is 60 mm.

The vibrator is located at the center of the base bottom as shown in Figure (1). It is composed of a rotating disk driven by ac motor, as shown in Figure (3), the disk has an unbalance mass of 20 grams, located at radius of 40 mm. The motor speed is 1800 rpm, so the frequency of the vibration is 30 Hz. and the maximum exiting force is about 20 Newton. The vibration is directed mainly to the vertical direction by using unidirectional elastic supports (rubber constrained layer) underneath the four columns which are carrying the system. The power consumed by the vibrator is about 60 watts, so that the daily electric consumption is about 1.44 KW h.

The basin outside surface is covered by two layers of foiled glass-wool of total thickness of 40 mm and rested on wooden plates of thickness 25 mm. The solar still is directed to the north-south direction.

1.2. System Design Parameters

The design parameters of the system are:

- Effective black area of basin is 2.064 m²;
- Net helical coil wires surface area is 4.75 m²;
- Helical coil diameter of 25 mm.
- Helical wire packing layer characteristic length is $l_w = 0.0375$ m
- Flat bottom basin characteristic length $l_b = 0.06$ m
- Copper wire with a diameter of 1.5 mm
- Density of wire material (copper) is 8890 kg/m³;
- The double-sloped angle is 30 deg. from horizontal.
- The basin height is 70 mm.
- The isolation thickness is 40 mm of wool glass of thermal conductivity of Kw.g = 0.038(W/mK). And wood of thickness 25 mm of thermal conductivity 0.04 W/mK.
- Vibrator frequency is 30 Hz.
- Exciting force is 20 N.
- Mass of the station is 150 kg.
- Mass of helical coiled wires is 6.55 kg.
- Density of polycarbonate glass sheet is 900 kg/m³.

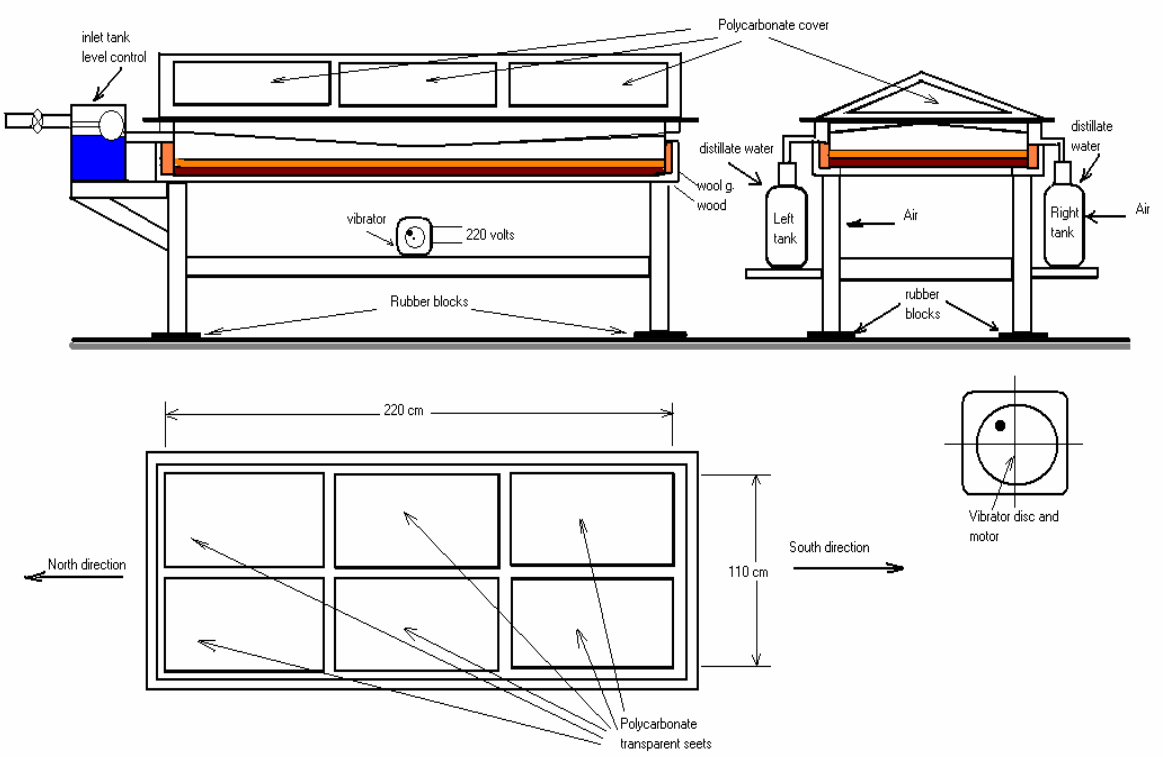

Fig. (1) Solar still configuration

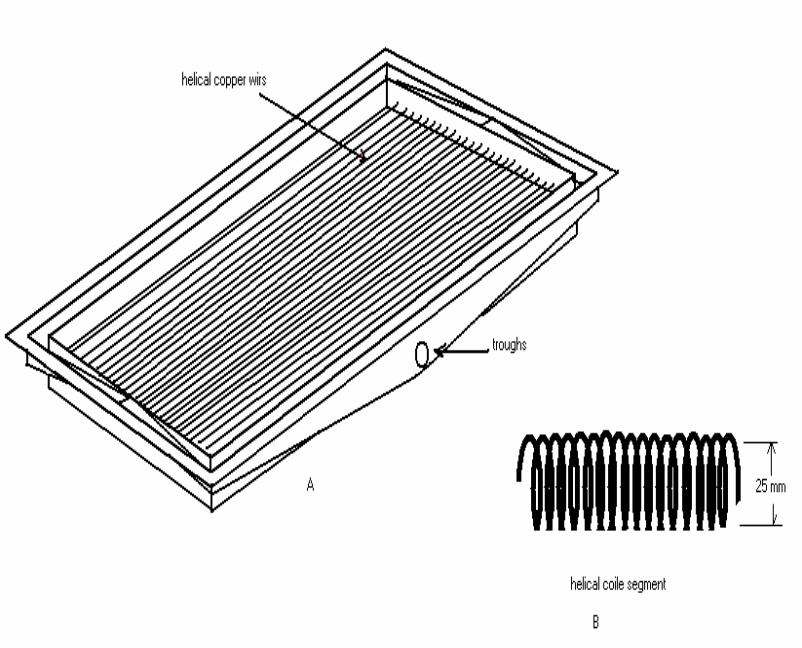

Fig. (2) Basin modified packed layer

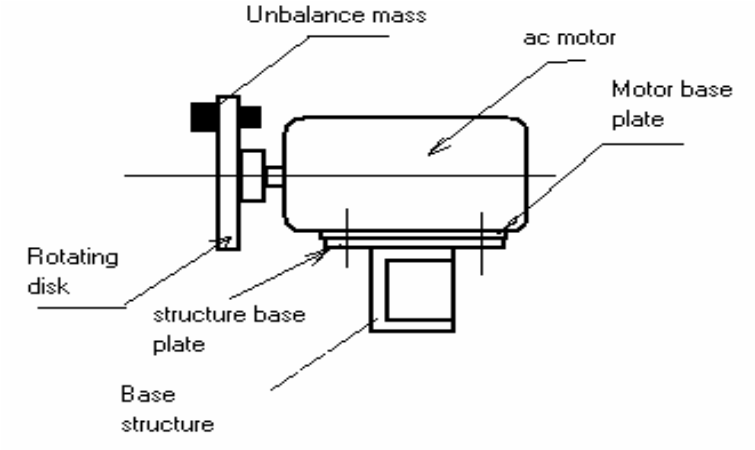

Fig. (3) Vibrator configuration

2. THEORETICAL ANALYSIS

Various designs of solar stills have been proposed in an attempt to improve the performance of solar stills. Hence the need for the characterization of various designs of solar stills is felt greatly to compare the relative performance of different solar stills. There are quite a few expressions given by various authors for internal convective heat transfer coefficient all based on Dunkle's relations who analyzed the enclosure as a parallel cavity.

The theoretical analysis is composed from three sections. The first section is the effect of the modified basin packed layer on the heat transfer parameters without vibratory

effect. The second section is the system dynamic modeling, and the third section is the effect of both helical wired packing layer and vibratory effect on the overall heat transfer coefficient.

2.1. Effect of the Modified Packed Layer

The conventional solar still performance is mathematically modeled by many investigators by utilizing the energy balance equation for the glass cover and water content in the basin, the energy balance will be, [5, 10, and12]:

2.1.1 The conventional solar still modeling

The energy balance for basin:

$$M_b \frac{\partial T_{1b}}{\partial t} = \alpha_b \tau_R I_s A_b - A_b [q_r + q_c + q_e + q_b]_1 \qquad \text{During sunlight} \qquad (1)$$

$$M_b \frac{\partial T_{2b}}{\partial t} = A_b [q_r + q_c + q_e + q_b]_2 \qquad \text{After sunset} \qquad (2)$$

The energy balance for glass cover:

$$A_g (q_r + q_c + q_e)_{g-b} = (q_r + q_c)_{g-a} \qquad \text{Steady state condition} \qquad (3)$$

$$M_g C_g \frac{\partial T_g}{\partial t} = \alpha_g \ I_s A_g - A_g [(q_r + q_c + q_e)_{g-b} - (q_r + q_c)_{g-a}] \qquad (4)$$

where:

M_b : thermal inertia of the brine water in the basin = $\rho_b l_b A_b C_{p_b}$

ρ_b : brine water density, kg/m³

l_b : brine water depth, = 0.06 m

A_b : basin area, m²

C_{p_b} : specific heat of the brine water, j/kg

α_b : absorptivity of brine water W/m²

$q_r, q_c, q_e and q_b$ are heat flow losses from the basin due to radiation, convection, evaporation, and the bottom, W/m²

I_s : solar insulation power, W/m².

M_g : thermal inertia of the polycarbonate glass cover $\rho_g l A_g c_{p_g}$

α_g : absorptivity of polycarbonate glass cover, W/m²

The rate of production of the conventional still is obtained by Dunkle formula [4] and Rubio et al. [11], by using the empirical formula of the free convection heat transfer, between the brine water surface and the glass cover surface, as follows:

$$m_c = \frac{16.276\times10^{-3}}{L_d} h_c \left(P_b - P_g\right)\times 3600 \tag{5}$$

$$h_c = 0.844\left[T_b - T_g + \frac{(P_b - P_g)T_b}{268.9\times10^3 - P_b}\right]^{1/3} \tag{6}$$

The internal free convective heat transfer, which is occurring between the basin black bottom and the brine water surface, may be obtained by the empirical free convection heat transfer when the heated surface is located in the upper direction, as follows, Holman [13] and Mills [14]:

$$N_{ui} = 0.14(G_r P_r)^{1/3} = 0.14(G_c)^{1/3}\left(\Delta T_{ic}\right)^{1/3}\times l_b \tag{7}$$

The heat transfer coefficient will be:

$$h_{ic} = \left[\frac{N_{ub}\times K_b}{l_b}\right] \tag{8}$$

$$h_{ic} = 0.14(G_c)^{1/3}\times K_b \times\left(\Delta T_{ic}\right)^{1/3} \tag{9}$$

And the rate of evaporation may be obtained by:

$$q_{ec} = h_{ci}(T_{bb} - T_{bs}) = 0.14(G_c)^{1/3}\times K_b \times(\Delta T_{ic})^{4/3} \tag{10}$$

Equating equation (9) with equation (5 and 6), the rate of evaporation can be found as:

$$q_{ec} = 0.14(G_c)^{1/3}\times K_b \times\left(\Delta T_{ic}\right)^{4/3} = 0.844\left[T_b - T_g + \frac{(P_b - P_g)T_b}{268.9\times10^3 - P_b}\right]^{1/3}\left(P_b - P_g\right) \tag{11}$$

And the rate of production can be obtained as follows:

$$\therefore m_c = \frac{q_{ec}}{L_d} = \frac{0.14(G_c)^{1/3}\times K_b}{L_d}\times(\Delta T_{ic})^{4/3} \tag{12}$$

where:
Subscript i means inside brine water.
m_c : rate of production of conventional still, kg / m² s

h_c : convective heat transfer coefficient, W / m² C°

G_r : Grashof number

P_r : Prandtl number

N_u : Nusselt number

G_c : constant of conventional still = $(G_r P_r)_c /(\Delta T_{ic})(l_b)^3$

$\Delta T_{ic} = T_{bb} - T_{bs}$ = Temperature difference between basin bottom surface and brine water surface respectively for conventional still.

L_d : distillate water latent heat = 2.35 Mj/kg

K_b : thermal conductivity of brine water, W/m C°

2.1.2 The helical wire packing layer modeling

The helical wire packing which is added to the basin is influencing the free convective heat transfer between the heating surface (helical wire packing layer surface) and the brine water surface. The helical wire packed layer is used to assist the desalination process during the sunrise and after the sunset, by increasing the basin water internal convective heat transfer, which may have significant impact on the thermal evaporation rate. So it may increase the rate of vaporization by working as a regenerative source of energy which may increase the nocturnal production

Thermal balance during sun light

$$M_w C_{pw} \frac{\partial T_{1w}}{\partial t} M_b C_{pb} \frac{\partial T_{1b}}{\partial t} = \alpha_w \tau_w I_s A_w + \alpha_b \tau_b I_s A_b - A_w [q_r + q_c + q_e + q_b]_{1w} \quad (13)$$

Thermal balance after sunlight

$$M_w C_{p_w} \frac{\partial T_{2w}}{\partial t} + M_b C_{p_b} \frac{\partial T_{2b}}{\partial t} = A_w [q_r + q_c + q_e + q_b]_{2w} \quad (14)$$

where:

q_{1w}, q_{1b} : the sum of radiated, convective, and evaporation of both helical wire and basin bottom, during sun light.

q_{lwb} : the sum of the external losses from helical wire and basin.

Subscripts w and b denote to helical wires packing and brine water, respectively.

C_{pw}, C_{pb} : Specific heats of helical wires and brine water, respectively.

M_w : thermal inertia of the helical wire packing layer = $m_w C_{p_w}$

$m_w and\ m_b$: Masses of the helical wires and brine water, respectively.

$A_{w,}$: surface area of helical wires, m²

$(\alpha\tau)_w and (\alpha\tau)_b$: absorptivity and transmissivity of the helical wires and brine water respectively.

$T_{w1,2}$: helical wire packing layer temperature, before and after sunset.

Equations (13) and (14) indicate that there is an increase in the thermal capacity of the still due to adding helical wire packed layer and also by increasing the basin brine water quantity. The increase in the thermal capacity of the still will increase the internal convective heat transfer rate q_{ew} from the helical wire packing surface to the brine water, which is utilized in the evaporation process by increasing the thermal evaporation flow rate q_{ew}. The modified internal convective heat transfer coefficient h_{cw} , due to helical wire, can be evaluated as a convection heat transfer from irregular surface. The configuration of the helical wire packing layer is shown in Figure (4), it can be modeled by using "Lienhard formula", as follows, Holman [13]:

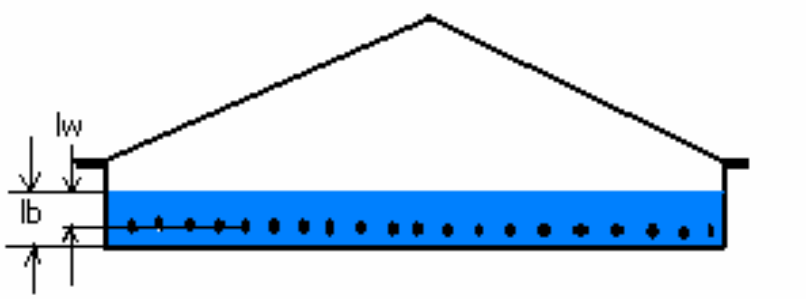

Fig. (4) Modified basin helical wire packing layer

$$h_{iw} = \frac{N_{uw} \times K_w}{l_w} = \left[\frac{0.52(G_r P_r)^{1/4} \times K_w}{l_w} \right] \tag{15}$$

$$\therefore q_{ew} = k_1 h_{iw} \Delta T_{iw} \tag{16}$$

$$m_w = \frac{q_{ew}}{L_d} = \left[\frac{0.52(G_w)^{1/4} \times K_w \times k_1}{L_d \times l_w^{1/4}} \times (\Delta T_{iw})^{1.25} \right] \tag{17}$$

If $K_b \approx K_w and G_w \approx G_c$, then, combining equations (12) and (17) we get:

$$\therefore \frac{m_w}{m_c} = 3.714 \times \frac{k_1 (\Delta T_{iw})^{1.25}}{(\Delta T_{ic})^{4/3} \times G_c^{1/12} \times l_w^{1/4}} \tag{18}$$

$$\therefore \frac{m_w}{m_c} = 0.48 \times \frac{k_1 (\Delta T_{iw})^{1.25}}{(\Delta T_{ic})^{4/3} l_w^{1/4}} \tag{19}$$

The average value of $G_c^{1/12} is 7.75$ for brine temperature range from 30 to 70 °C, and assuming that the temperature gradient in the basin water depth is linear, and then the

ratio between the temperature differences in cases of conventional and after added helical wire packing layer will be proportional to the depths, as follows:

$$\frac{\Delta T_{ic}}{l_c} = \frac{\Delta T_{iw}}{l_w} \tag{20}$$

where:

l_b : basin characteristic length, is the distance a particle travels in the boundary layer, basin water depth, m

l_w : helical wire characteristic length, average water depth, m

K_w : thermal conductivity of the brine water in the boundary layer of the helical wire packing surface, W/m C°

$k_1 = \frac{A_w}{A_b}$ the ratio of helical wire surface area and the basin area.

ρ_d : distillate density, kg/m

2.2. System Dynamic Modeling

The aim of the system modeling from the theory of vibration point of view is to determine the dynamic parameters of the system elastic components, such that elastic foundation supports, the helical wires packed bed, and polycarbonate transparent glass sheet covers which magnify the transmissibility of the harmonic excitation. The system dynamically is modeled through two steps, the first step is the vibratory excitation and foundation support-system modeling; the second step is the system-helical coiled wires and system-glass sheets modeling. The first modeling is based on the excitation effect of the vibratory harmonic forced motion on the system structure and foundation supports. The second modeling is based on the vibration transmissibility principle. The system modeling diagram is shown in Figure (5).

Considering the system and foundation supports as spring mass system constrained to move in the vertical direction and excited by a rotating unbalance mass (m). By letting *y* be the displacement of the no rotating mass (M-m), the equation of motion is then [15]:

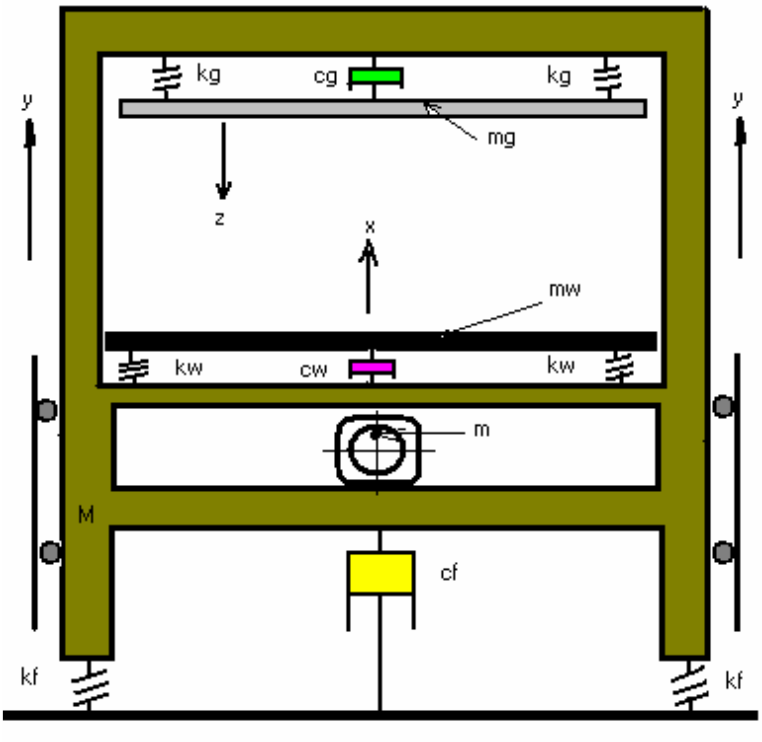

Fig. (5) System dynamic modeling

$$(M-m)\ddot{y}+\frac{md^2\left(y+e\sin\omega_v t\right)}{dt^2}=k_f\,y-c_f\,\dot{y} \qquad (21)$$

where:

k_f : the elastic foundation stiffness, N/m

c_f : the elastic foundation damping coefficient, N sec/m

ω_v : the frequency of the vibrator, rad/sec

M : the mass of the structure, kg

m : the unbalance mass of the vibrator, kg

e : the radius of the unbalance mass center of gravity 0.04 m

This can be arranged to:

$$M\ddot{y}+c_f\,\dot{y}+k_f\,y=\left(me\omega_v^2\sin\omega_v t\right) \qquad (22)$$

The solution of equation (8) includes two parts, unsteady state solution (transient periods) and steady state solution. In our case the steady state solution part is considered, it will be as:

$$Y = \frac{me\left(\omega_v / \omega_{nf}\right)^2}{M\sqrt{\left[1-\left(\frac{\omega_v}{\omega_{nf}}\right)^2\right]^2 + \left(2\zeta_f \frac{\omega_v}{\omega_{nf}}\right)^2}} \tag{23}$$

where:

Y : the system displacement amplitude, m

ω_{nf} : the natural frequency of the system-foundation, rad/sec

ζ_f : the damping ratio of the foundation = cf/crf

c_{rf} : elastic foundation critical damping coefficient, Nm/sec

The excitation transmissibility of the helical coiled wires can be evaluated by the transmissibility dimensionless equation as follows [15]:

$$X / Y = \frac{\sqrt{\left[1+\left(2\zeta_w \frac{\omega_v}{\omega_{nw}}\right)^2\right]}}{\sqrt{\left\{\left[1-\left(\frac{\omega_v}{\omega_{nw}}\right)^2\right]^2 + \left[2\zeta_w \frac{\omega_v}{\omega_{nw}}\right]^2\right\}}} = TR_w \tag{24}$$

where:

X : maximum displacement amplitude of the helical wires, m

TR_w : transmissibility ratio for helical wires

ω_{nw} : natural frequency of the helical wires = $\sqrt{k_w / m_w}$, rad/sec

m_w : mass of helical wires, kg

k_w : stiffness of the helical wires, N/m

c_w : damping coefficient of helical wires, N sec/m

ζ_w : damping ratio of the helical wires = c_w / c_{rw}

c_{rw} : elastic damping coefficient of the helical wires, N sec/m

Then the helical wires excitation displacement amplitude can be obtained as follows:

$$X = \frac{me\left(\frac{\omega_v}{\omega_{nf}}\right)^2 \sqrt{\left[1+\left(2\zeta_w \frac{\omega_v}{\omega_{nw}}\right)^2\right]}}{M\sqrt{\left\{\left[1-\left(\frac{\omega_v}{\omega_{nw}}\right)^2\right]^2 + \left[2\zeta \frac{\omega_v}{\omega_{nw}}\right]^2\right\}\left\{\left[1-\left(\frac{\omega_v}{\omega_{nf}}\right)^2\right]^2 + \left[2\zeta_f \frac{\omega_v}{\omega_{nf}}\right]^2\right\}}} \tag{25}$$

And for glass covers, the excited displacement amplitude will be evaluated by the same transmissibility equation as follows:

$$Z/Y = \frac{\sqrt{\left[1+\left(2\zeta_w \frac{\omega_v}{\omega_{ng}}\right)^2\right]}}{\sqrt{\left\{\left[1-\left(\frac{\omega_v}{\omega_{ng}}\right)^2\right]^2+\left[2\zeta_w \frac{\omega_v}{\omega_{ng}}\right]^2\right\}}} = TR_g \qquad (26)$$

where: Z is the displacement amplitude of the glass covers, and the suffix (g) is denoting to the glass covers.

Similarly, the glass covers displacement amplitude Z is found as:

$$Z = \frac{me\left(\frac{\omega_v}{\omega_{nf}}\right)^2 \sqrt{\left[1+\left(2\zeta_w \frac{\omega_v}{\omega_{ng}}\right)^2\right]}}{M\sqrt{\left\{\left[1-\left(\frac{\omega_v}{\omega_{ng}}\right)^2\right]^2+\left[2\zeta \frac{\omega_v}{\omega_{ng}}\right]^2\right\}\left\{\left[1-\left(\frac{\omega_v}{\omega_{nf}}\right)^2\right]^2+\left[2\zeta_f \frac{\omega_v}{\omega_{nf}}\right]^2\right\}}} \qquad (27)$$

Where:

TR_g : Transmissibility ratio for polycarbonate cover

ω_{ng} : the natural frequency of the polycarbonate cover = $\sqrt{k_g / m_g}$, rad/sec

m_g : the mass of helical wires, kg

k_g : the stiffness of the polycarbonate cover, N/m

c_g : the damping coefficient of polycarbonate cover, N sec/m

ζ_g : the damping ratio of the polycarbonate cover = c_g / c_{rg}

c_{rg} : polycarbonate cover critical damping coefficient, N sec/m

There were different phase angles between the vibrator harmonic and the exited parts of the system; it had no effect on our application.

Equations (24) and (26) represent the transmissibility of the vibration to the helical wires packed layer and polycarbonate glass cover. They indicate that the maximum exciting displacement will occur, when the damping coefficients of the foundation supports (ζ_f) and the excited elements (ζ_w ζ_g) are very small and almost the same. And also, when the natural frequencies of these parts (ωnf, ωnw ωng) are very close to the

vibrator harmonic frequency (ω_v) or may be equal to it. So, sharpening of resonance will occur [16]. This case will be very close to the resonance of the system, but due to the lower excitation power with respect to the system stiffness, no damage is expected. The amplitude displacements of the helical wires and polycarbonate glass covers will be calculated using equations (23) and (27).

The polycarbonate glass sheets can stand strongly to the excited displacement without breaking like glass this is due to its high elasticity and its very low damping coefficient.

Neglecting the higher order values of ζ_f, ζ_w, and ζ_g because of their very small values, then; the peak of the transmissibility will occur when [15].

$\omega_v / \omega_{nf} = \sqrt{1-2\zeta_{nf}}$, similarly $\omega_v / \omega_{nw} = \sqrt{1-2\zeta_{nw}}$ and $\omega_v / \omega_{ng} = \sqrt{1-2\zeta_{nfg}}$

The vibrating helical wires will induce traveling harmonic waves in the brine water in the normal direction of the helical wires motion [17]; these traveling waves have a value depending on the vortex shedding in the wake of the helical wires. Evaluating the relative velocity between brine water and helical wires will be getting more complex; so, we will consider only the wire velocity, it can be calculated as a root mean square value of the peak velocity ($V_{w\max}$) as:

$$V_{wm} = X\omega_w \cos\omega t = \frac{X\omega_w}{\sqrt{2}} \approx \omega_v \frac{X}{\sqrt{2}} \qquad (28)$$

The helical wires velocity is a function of the harmonic excitation frequency, and it will magnify the convection part of heat transfer in the energy balance process when working with the vibrator.

2.3. Vibratory Harmonic Motion Effect

The effects of the vibratory harmonic motion on the still performance is divided into three phases, the first phase is the thermodynamic analysis. The second phase is the dynamic effect of the glass cover on the droplet collecting quality.

2.3.1 Thermodynamic Analysis

The helical wires packing layer is considered as a regular shape wire matrix (porous media) and when excited by the vibratory harmonic motion a forced convection heat transfer process will exist with the surrounded brine water, it can be modeled as the mixed convection-turbulent according to the value of Reynolds no. process which correlated by "Metais formula", Holman [13], as follows:

For $10^3 \le R_e \le 10^4$ and Gr Pr D/L > 10^6 (29)

$$N_u = 4.69 R_e^{0.27} P_r^{0.21} G_r^{0.07} \left(\frac{d_h}{l_w} \right)^{0.36} \tag{30}$$

Reynolds number, Re, may found by using equation (28), as follows:

$$R_e = \rho_b \frac{X\omega \cos \omega_w t}{\mu_b} \times d_h = \rho_b \frac{X d_h}{\mu_b \sqrt{2}} = \rho_b \frac{U_{wm} d_h}{\mu_b} \tag{31}$$

And the evaporation thermal flow rate will be:

$$q_{evib} = \frac{k_2 \times N_u K_b}{l_w} \times \Delta T_{ivib} \tag{32}$$

where:

μ_b : the viscosity of brine water in boundary layer of helical wire, kg/m s.

d_h : Hydraulic diameter, is equal to the helical wire diameter, m

The increasing ratio of the thermal evaporation rate will be obtained by dividing equation (32) by equation (17), as follows:

$$\frac{m_{vib}}{m_w} = \frac{12.56 \times G_r^{0.07} \times k_2 \times l_w^{1/4} (T_{vib})}{0.52 \times G_w^{1/4} l_w \times k_1 \times (\Delta T_{iw})^{5/4}} \tag{33}$$

$G_r^{0.07}$ no. can be taken as a constant = 2.9 with accuracy of 3% in the range of brine water temperature from 30 to 70 °C.

$$m_{vib} / m_w = 117 \times \frac{k_2 \times R_e^{0.27}}{k_1 \times G_w^{1/4} (\Delta T_{iw})^{1/4}} \tag{34}$$

where:

ΔT_{ivib} is the boundary layer temperature difference when vibration is applied, it can be assumed that it equal to $\approx \Delta T_{iw}$.

k_2 is the wavy surface area ratio, $= A_{vib} / A_b \approx k_1$

2.3.2. Droplet Collecting Quality.

The droplets of the condensed water vapor on the polycarbonate glass cover are suffering from the surface tension force which opposing gravity force component along the glass cover slope. The dynamic effect of the glass cover will generate an additional inertia force applied on the droplet boundary in addition to the gravity force component, so the droplet will slide easy before it became as the previous size.

The sliding forces F_1 and F_2 without and with vibration, as shown in Figure (6, A and B), is defined as follows:

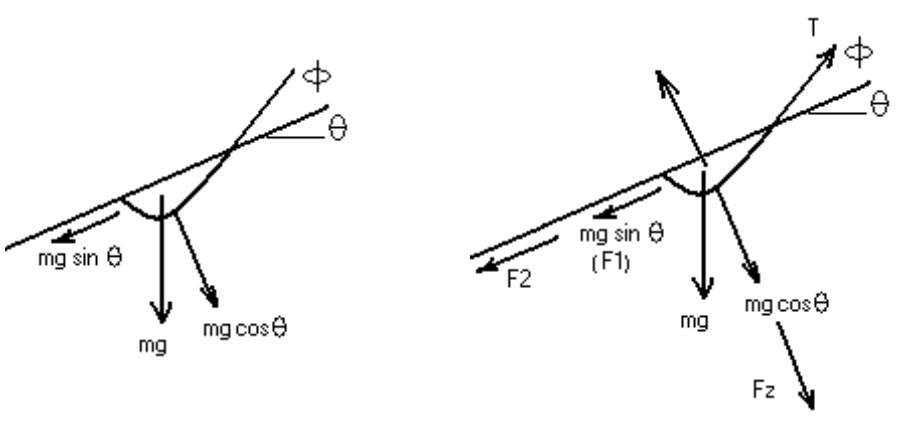

A- without vibration **B- with vibration**

Fig. (6) Sliding force analysis

$$F_1 = mg \sin\theta \tag{35}$$

The sliding insipient of the condensed droplet will be:

$$F_1 \geq T \cos\phi \tag{36}$$

Where T is the net surface tension force acting around the droplet circumference,

$$T = \pi d\sigma$$
$$F_1 \geq \pi d\sigma \cos\phi \tag{37}$$

The force generated due to vibration will be,

$$F_z = \pm m\ddot{z} \cos\omega t \tag{38}$$

The additional sliding force will be:

$$F_2 = \frac{mzZ\omega^2 \cos\theta \sin\theta}{\sqrt{2}} \tag{39}$$

Then, the total force will be,

$$F = F_1 + F_2 = m \sin\theta \left(g + \frac{Z\omega^2 \cos\theta}{\sqrt{2}} \right) \tag{40}$$

The increase in the sliding force will be:

$$\frac{F_1 + F_2}{F_1} = 1 + \frac{Z\omega^2 \cos\theta}{g\sqrt{2}} \approx 1.22 \qquad (41)$$

The increase of the collecting condensation is proportional to the increase in the sliding force. Then, the total vibratory motion effect will be obtained by combining equations (34) and (41).

3. THEORETICAL RESULTS AND VALIDATION

The theoretical calculation results of the of the thermal modeling relations is started by constructing the thermal boundary layer temperature difference of the conventional solar still, which is derived by equation (11) at different temperature differences between brine water surface and internal glass cover, as shown in Figure (7). The figure indicates that the boundary layer temperature difference increases with increasing the brine water surface temperature, also increases with increasing temperature difference with the glass cover.

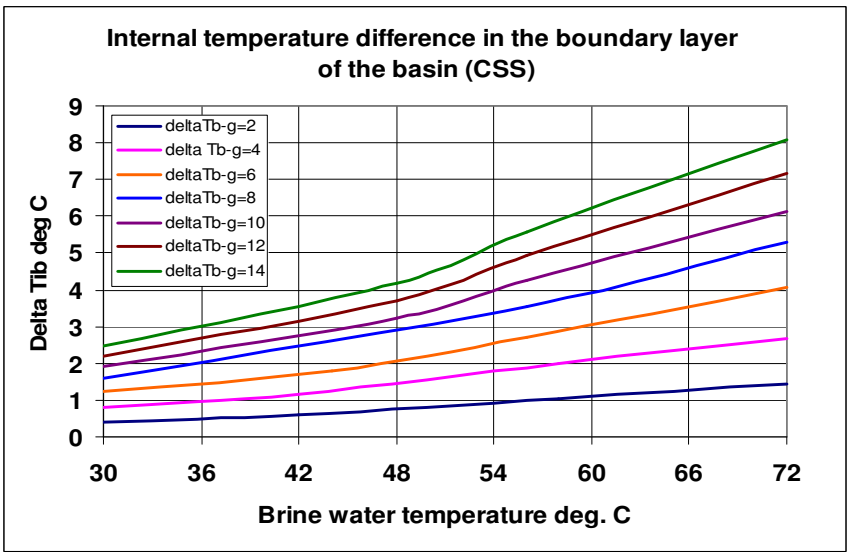

Fig. (7) Boundary layer temperature difference in the flat bottom basin, obtained by equation (11)

3.1. Helical Wire Packing Evaluation

The helical wire packing performance is evaluated, first, by obtaining the new boundary layer temperature differences, equation (20), which are corresponding to the basin water- glass cover temperature differences, as shown in Figure (8). It has the same trend as the flat bottom basin.

Then the rate of production (PRP) is obtained by using equation (19). Figure (9) shows the variation of the rate of production (PRP) with varying the basin water temperature and glass cover difference temperatures, which indicates that the PRP decreases with increasing the brine water temperature. It has an average increasing value of about 27% more than the CSS at the same thermal conditions. This value comes in good agreement when compared with the experimental results of CSS which obtained by Zienab et al. [10] and the experimental measurements of the modified solar still which indicated in part-1 by the author [1]. As shown in Figures (10 and 12), the maximum rate of production ratio (PRP) is occurred after sunset (night) when the temperature of the brine water is decreased to the lower value.

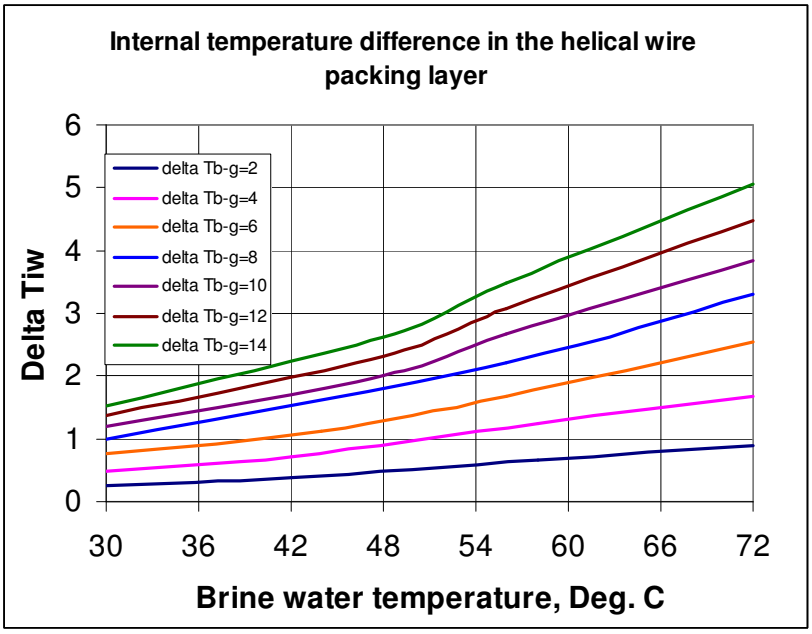

Fig. (8) Boundary layer temperature difference in the basin with helical wire packing layer, obtained by equation (21)

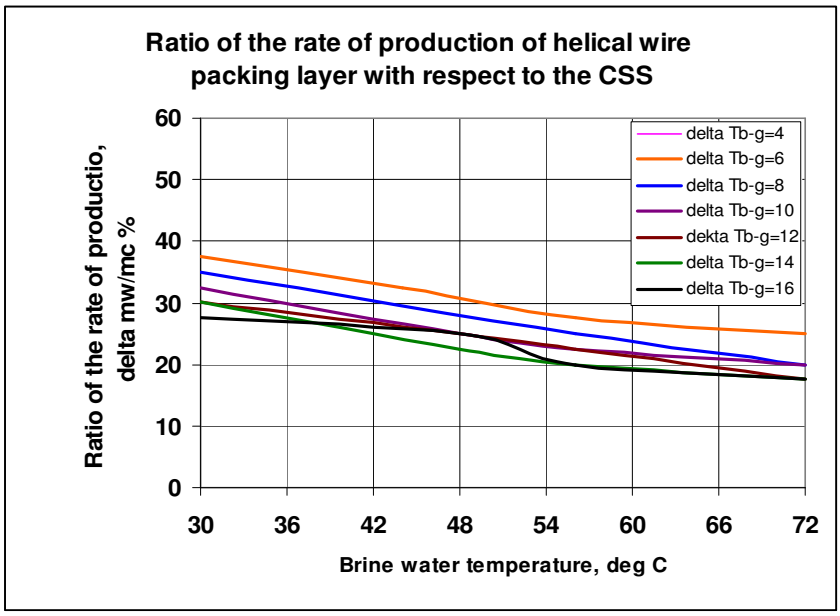

Fig. (9) Variation of the rate of production ratio of the helical wire packing with the brine water surface temperature

3.2. Vibratory Harmonic Effect Evaluation

The performance of the solar still with vibratory motion effect is calculated by combining equations (34 and 41). The rate of production ratio is obtained at different brine water temperatures together with glass cover difference temperatures. Figure (11) shows that the rate of production ratio is decreasing with increasing the brine water temperature and with increasing the temperature difference of the glass cover. It behaves the same as obtained before for helical wire packing layer without vibration effect. Figure (12) shows the experimental measurements of the rate of production and the accumulated productivity ratios with and without vibration effect together, as measured by the author in part-1, with typical measured temperatures of both basin water and glass cover as measured by Aboul-Enein et al. [6]. It is obvious that the rate of production ratio is increasing with decreasing the brine water temperature, which is occur after sun set until sun rise. The validation is carried out by comparing three experimental points 1, 2, and 3, as shown in Figure (11). The percentage deviations between the experimental measurements and theoretically calculated values of the rate of the production at the selected points are shown in Table (1). The deviation is ranged between 3.3 % and 6.5%.

Table (1) Comparison between measured and theoretically calculated values of production rate ratios

Comp. point no.	Water Temp (ºC)	Water-glass dif. Temp. (ºC)	Rate of production ratio		Deviation (%)
			Exp.	Theor.	
1	32	3	2.22	2.3	3.6
2	40	8	1.7	1.81	6.5
3	47	11	1.5	1.55	3.3

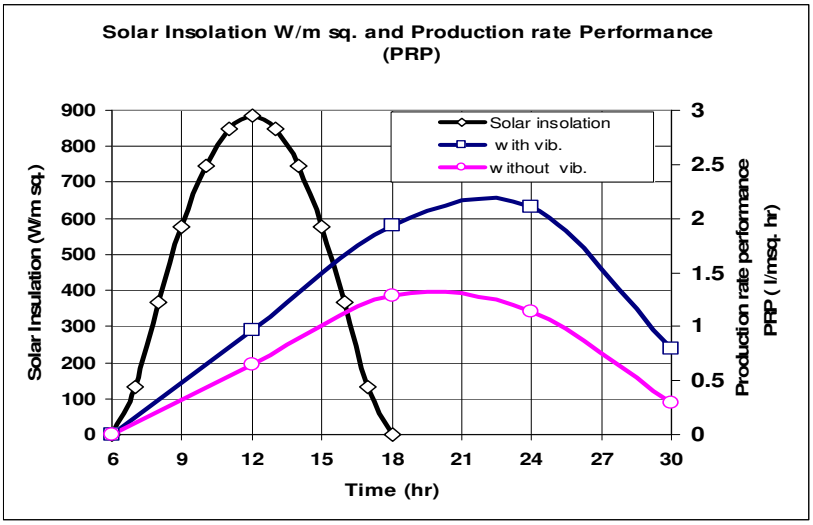

Fig. (10) Experimental measurements of rate of production with and without vibration with respect to the solar insulation

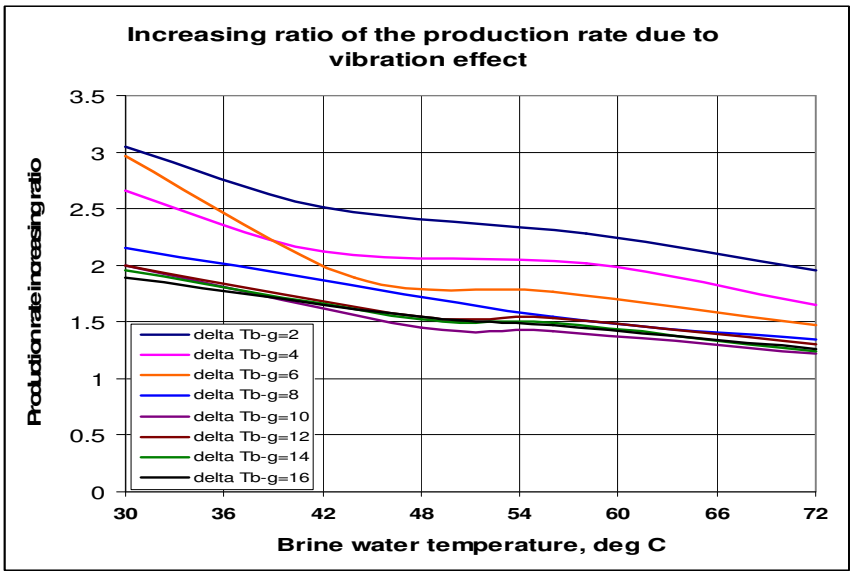

Fig. (11) Variation of the rate of production increasing ratio with vibration applied as obtained by equation (35)

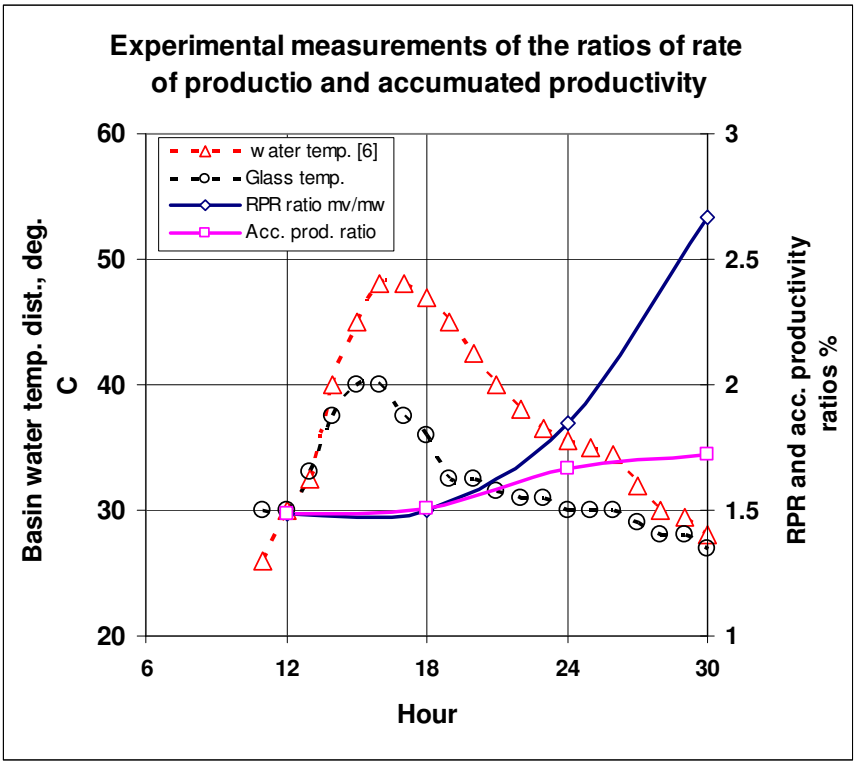

Fig. (12) Experimental measurements of the rate of production and accumulated productivity ratios and typical basin water temperature distribution, Aboul-Enein et al. [6]

4. CONCLUSION

The theoretical analysis of a new concept basin type solar still with added helical wires packing layer subjected to a vibratory effect is presented.

The rate of production ratio (PRP) due to adding the helical wire packing layer is modeled by using the empirical relations of the free convection heat transfer in order to correlate the thermal boundary layer temperature gradient of the basin in the cases of flat bottom and helical wire packing layer with and without vibratory effects.

The system dynamics is analyzed and modeled based on the transmissibility equation for evaluating the periodic motions of the helical wired packing layer and the condensing polycarbonate glass cover. The effect of these harmonic motions on the heat transfer coefficient is correlated by considering the increasing term of the turbulence motion in the basin water, and taking into account additional inertia forces which affecting the insipient of the condensed droplets on the polycarbonate glass cover by advancing sliding conditions.

The theoretically calculated results of the rate of production ratios of the solar still when adding helical wired packing layer, with and without vibration; is compared with

the experimental results and the validation comes in good agreement for both the trend directions and the specific values.

The deviation of the theoretically calculated results is found about +7% and +11.1% at low and high basin water temperatures respectively, as compared with the experimental results discussed in part-1, by the author [1] and Aboul-Enein et al. [6].

REFERENCES

[1] Khaled. M. S. Eldali1, "New Concept for Improving Solar Still Performance by Using Vibratory Harmonic Effect**,** Experimental Prediction, Part-1". Thirteenth International Water Technology Conference, 12-15 March 2009 Hurghada, Egypt.

[2] Singh AK, Tiwari GN, Sharma PB, Khan E. "Optimization of orientation for higher yield of solar still for a given location". Energy Conversion and Management 1995; 36 (3):175–81.

[3] Sharma VB, Mullick SC. "Estimation of heat-transfer coefficients, the upward heat flow, and evaporation in a solar still". ASME Journal of Solar Energy Engineering 1991; 113:36–41.

[4] Dunkle RV., "Solar water distillation: the roof type still and a multiple effect diffusion still". In: International Developments in Heat Transfer, Int. Heat Transfer Conference, University of Colorado. 1961. p. 895–902 Part 5.

[5] D. Mowla and G. Karimi, "Mathematical Modelling of Solar Stills in Iran", Solar Energy, Vol. 55, No. 5, pp. 389-393, 1995.

[6] S. Aboul-Enein, A A. El-Sebaii and E. EL-Bialy, "Investigation of a Single-Basin Solar Still with Deep Basins", Renewable Energy, Vol. 14, Nos. l-4, pp. 299-305, 1998.

[7] G. N. Tiwari and M. A. Noor, "Characterisation of Solar stills", Inr. J. Solar Energy, 1996, Vol. 18, pp. 147-171, 1996.

[8] Hiroshi Tanaka, Yasuhito Nakatake, "Factors influencing the productivity of a multiple-effect diffusion-type solar still coupled with a flat plate reflector", Desalination 186 (2005) 299–310

[9] Hiroshi Tanaka, Yasuhito Nakatake, "Theoretical analysis of a basin type solar still with internal and external reflectors", Desalination 197 (2006) 205-216.

[10] Zeinab S. Abdel-Rehim, Ashraf Lasheen, "Improving the Performance of Solar Desalination Systems", Renewable Energy 30 (2005) 1955–1971.

[11] Eduardo Rubio-Cerda, Miguel A. Porta-Ga´ndara, Jose´ L. Ferna´ndez-Zayas, Technical note, "Thermal performance of the condensing covers in a triangular solar still", Renewable Energy 27 (2002) 301–308.

[12] A. A. Fatani and G. M. Zaki, "Analysis of Roof Type Solar Stills with Assisting External Condensers", Inr. J. Solar Energy, 1995, Vol. 17, pp. 27-39.

[13] J. P. Holman," Heat Transfer", 8th Edition, International Edition, McGraw-Hill, 1997.

[14] A. F. Mills, "Heat Transfer", Richard D. Irwin, Inc., 1992.

[15] William T. Thomson, Theory of vibration with applications, Fourth Edition, Chapman & Hall, Prentice-Hall, Inc, Englewood Cliffs, New Jersey, USA, ISBN 0412546205, 1993

[16] Leonard Meirovitch, "Fundamental of vibrations", Publisher: Tomas Casson, McGraw-Hill Higher Education, ISBN 0070413452.

[17] Robert D. Blevins, "Flow-induced vibration", published by Van Nostrand Reinhold Company, ISBN: 0-442-20828-6, 1977.